1-1-2015

Descriptions of the dental remains of Homo floresiensis

Yousuke Kaifu
National Museum of Nature and Science, Japan, kaifu@kahaku.go.jp

Reiko T. Kono
National Museum of Nature and Science, Japan

Thomas Sutikna
University of Wollongong, ts788@uowmail.edu.au

E Wahyu Saptomo
University of Wollongong

- Jatmiko
University of Wollongong

See next page for additional authors

Descriptions of the dental remains of Homo floresiensis

Abstract

Dental remains of Homo floresiensis excavated during 2002-2004 at Liang Bua, Flores, Indonesia, consist of one partial maxillary dentition, two nearly complete mandibular dentitions, and four isolated teeth. We present here morphological descriptions of all these specimens and report aspects of their dentition, occlusion, and oral health condition. This dental assemblage represents probably five but possibly four or six individuals. These different individuals share similar dental characteristics, supporting the view that the Liang Bua H. floresiensis assemblage represents a single population. We also reassess the previous claims for primitive and modern aspects of the H. floresiensis teeth. The previous studies reached conflicting conclusions: some researchers claim that these teeth are fully modern, whereas others highlight premolar and other morphologies that suggest their direct evolutionary link with the African earliest form of Homo or Australopithecus rather than with H. erectus. Neither of these views are supported. The H. floresiensis teeth exhibit a mosaic of primitive, derived, and unique characters, with the reported primitive aspects broadly comparable to the morphologies observed in H. erectus sensu lato. Although a more comprehensive comparative analysis is needed to fully illustrate dental morphological affinities of this dwarfed hominin species, we find no grounds for the hypothesis that H. floresiensis originated from the small-bodied, primitive hominins such as H. habilis sensu lato.

Keywords

Homo floresiensis, Flores, Indonesia, dental morphology

Disciplines

Medicine and Health Sciences | Social and Behavioral Sciences

Publication Details

Kaifu, Y., Kono, R. T., Sutikna, T., Saptomo, E. Wahyu., Jatmiko, , Awe, R. Due. & Baba, H. (2015). Descriptions of the dental remains of Homo floresiensis. Anthropological Science, 123 (2), 129-145.

Authors

Yousuke Kaifu, Reiko T. Kono, Thomas Sutikna, E Wahyu Saptomo, - Jatmiko, Rokus Awe Due, and Hisao Baba

ANTHROPOLOGICAL SCIENCE
Vol. 123(2), 129–145, 2015

Descriptions of the dental remains of *Homo floresiensis*

Yousuke KAIFU[1,2]*, Reiko T. KONO[1], Thomas SUTIKNA[3,4], E. Wahyu SAPTOMO[4,3], JATMIKO[4,3], Rokus Due AWE[4,3]**, Hisao BABA[1]

[1]*Department of Anthropology, National Museum of Nature and Science, 4-1-1 Amakubo, Tsukuba-shi, Ibaraki 305-0005, Japan*
[2]*Department of Biological Sciences, The University of Tokyo, 3-1-1 Hongo, Bunkyo-ku, Tokyo 113-0033, Japan*
[3]*Centre for Archaeological Science, University of Wollongong, Northfields Avenue, Wollongong, NSW 2522, Australia*
[4]*The National Research and Development Centre for Archaeology, Jl. Raya Condet Pejaten No 4. Jakarta 12510, Indonesia*

Received 19 December 2014; accepted 1 May 2015

Abstract Dental remains of *Homo floresiensis* excavated during 2002–2004 at Liang Bua, Flores, Indonesia, consist of one partial maxillary dentition, two nearly complete mandibular dentitions, and four isolated teeth. We present here morphological descriptions of all these specimens and report aspects of their dentition, occlusion, and oral health condition. This dental assemblage represents probably five but possibly four or six individuals. These different individuals share similar dental characteristics, supporting the view that the Liang Bua *H. floresiensis* assemblage represents a single population. We also reassess the previous claims for primitive and modern aspects of the *H. floresiensis* teeth. The previous studies reached conflicting conclusions: some researchers claim that these teeth are fully modern, whereas others highlight premolar and other morphologies that suggest their direct evolutionary link with the African earliest form of *Homo* or *Australopithecus* rather than with *H. erectus*. Neither of these views are supported. The *H. floresiensis* teeth exhibit a mosaic of primitive, derived, and unique characters, with the reported primitive aspects broadly comparable to the morphologies observed in *H. erectus sensu lato*. Although a more comprehensive comparative analysis is needed to fully illustrate dental morphological affinities of this dwarfed hominin species, we find no grounds for the hypothesis that *H. floresiensis* originated from the small-bodied, primitive hominins such as *H. habilis sensu lato*.

Key words: *Homo floresiensis*, Flores, Indonesia, dental morphology

Introduction

Homo floresiensis is a diminutive, primitive hominin found from Flores, eastern Indonesia (Brown et al., 2004; Morwood et al., 2004, 2005). The skeletal remains of this new species are known from the Late Pleistocene strata at Liang Bua, a limestone cave on the island. Morphology of its cranium, endocast, mandible, shoulder girdle, pelvis, limb bones, hand, and foot have been described, analyzed, and interpreted (Brown et al., 2004; Morwood et al., 2005; Falk et al., 2005, 2009; Argue et al., 2006, 2009; Larson et al., 2007, 2009; Tocheri et al., 2007; Gordon et al., 2008; Baab and McNulty, 2009; Brown and Maeda, 2009; Holliday and Fransiscus, 2009, 2012; Jungers et al., 2009a, b; Lyras et al., 2009; Aiello, 2010; Kaifu et al., 2011; van Heteren, 2012; Baab et al., 2013; Jungers, 2013; Kubo et al., 2013; Orr et al., 2013; Daegling et al., 2014). However, not all the dental remains have been described in sufficient detail, and there even exists controversy as to whether the dental morphology of *H. floresiensis* is primitive or modern (Jacob et al., 2006; Brown and Maeda, 2009).

In this paper, we provide detailed morphological description for all the dental materials of *H. floresiensis* excavated during the 2002–2004 field seasons at Liang Bua (Morwood and Jungers, 2009). Most of the mandibular teeth of *H. floresiensis* have been described by Brown and Maeda (2009), but we here describe these materials again based on our own observation of the original specimens and high-resolution micro-CT scans that were not available to the previous researchers. We also reassess the previous claims for primitive and modern aspects of the *H. floresiensis* teeth.

Materials and Methods

The Liang Bua dental collection: 2002–2004

Bony and dental remains belonging to multiple individuals have been excavated and reported from the Pleistocene levels at Liang Bua (Morwood and Jungers, 2009; Morwood et al., 2009). In this collection, the cranium (LB1/1) and mandible (LB1/2) of the individual LB1, as well as the mandible (LB6/1) from another individual preserve their dentitions. Additionally, there are four isolated teeth as shown in Table 1 and illustrated in Figure 1, Figure 2, Figure 3, and

* Correspondence to: Yousuke Kaifu, Department of Anthropology, National Museum of Nature and Science, Tokyo, 4-1-1 Amakubo, Tsukuba-shi, Ibaraki 305-0005, Japan.
E-mail: kaifu@kahaku.go.jp
** deceased

Published online 18 July 2015
in J-STAGE (www.jstage.jst.go.jp) DOI: 10.1537/ase.150501

Table 1. Inventory and measurements of the *H. floresisensis* dental remains from Liang Bua

Specimen	Individual	Tooth	Side	Sector	Spit	Wear	Crown diam.			Cervical diam.[a]		Root length
							MD	MD corrected	BL	MD	BL	
Maxilla												
LB15/2	LB15/2	I^1	L	III	51	7	—	—	≥6.2	5.2	6.2	12–13
LB1/1	LB1	C^1	R	VII	59	5	8.1	—	8.0	*(6.1)*	*7.8*	*20.3*
LB1/1	LB1	C^1	L	VII	59	6[b]	7.8	—	7.8	*6.4*	*7.7*	*19.8*
LB1/1	LB1	P^3	R	VII	59	3	6.8	7.0	9.7	*4.7*	*9.4*	*15.9*
LB1/1	LB1	P^3	L	VII	59	4	6.9	7.0	8.8	*5.0*	*8.6*	*14.0*
LB1/1	LB1	P^4	R	VII	59	3	6.9	6.9	(8.8)[c]	*5.1*	*(8.1)*	*16.0*
LB1/1	LB1	P^4	L	VII	59	4	7.1	7.1	(8.9)[c]	*5.0*	*8.7*	*14.9*
LB1/1	LB1	M^1	R	VII	59	5	9.3	9.3	11.3	*7.4*	*10.9*	*12.8, 13.4, 11.9*[d]
LB1/1	LB1	M^1	L	VII	59	5	9.0	9.0	11.5	—	—	—
LB1/1	LB1	M^2	R	VII	59	4	9.4	9.4	10.9	*7.4*	*10.1*	*13.7, 13.1, 12.3*[d]
LB1/1	LB1	M^2	L	VII	59	4	9.3	9.3	10.8	*7.3*	*10.3*	—
Mandible												
LB1/1	LB1	I_1	L	VII	59	6	3.8	—	5.0	*3.5*	*5.0*	*14.0*
LB6/14	LB6/1?	I_1	L	XI	53	5	3.7	—	5.0	3.3	5.0	12.2
LB1/2	LB1	I_2	R	VII	59	4	4.7	—	5.7	*4.0*	*5.8*	*14.3*
LB1/2	LB1	I_2	L	VII	59	5.5	4.3	—	5.7	*3.8*	*5.7*	—
LB6/1	LB6/1	I_2	R	XI	51	4	4.5	—	5.2	—	5.2	—
LB1/2	LB1	C_1	R	VII	59	4.5	6.7	—	7.4	*6.2*	*7.2*	*17.2*
LB1/2	LB1	C_1	L	VII	59	5.5[b]	6.7	—	7.4	*6.0*	*7.2*	*16.4*
LB6/1	LB6/1	C_1	R	XI	51	4	6.3	—	6.7	—	6.5	—
LB6/1	LB6/1	C_1	L	XI	51	4	6.1	—	6.7	5.2	6.6	—
LB1/2	LB1	P_3	R	VII	59	4	8.6	8.6	8.5	*6.4*	*8.3*	*12.0*
LB1/2	LB1	P_3	L	VII	59	5	8.5	8.5	8.4	*6.6*	*8.5*	*13.6*
LB2/2	LB2/2	P_3	L	IV	43D	4	8.6	8.6	8.7	7.0	8.5	12.4
LB6/1	LB6/1	P_3	R	XI	51	4	8.0	8.2	7.8	—	—	—
LB6/1	LB6/1	P_3	L	XI	51	4	8.0	8.2	7.8	6.6	7.8	(10.7)
LB6/1	LB6/1	P_4	R	XI	51	4	6.6	6.7	7.8	—	—	—
LB6/1	LB6/1	P_4	L	XI	51	4	6.1	(6.7)	7.7	5.0	6.7	13.2
LB15/1	LB15/1	P_4	R	III	48	4	7.2	(7.7)	8.5	5.9	7.7	14.3
LB1/2	LB1	M_1	R	VII	59	3.5	9.5	9.6	10.6	*8.5*	*9.1*	*12.3, 12.5*[e]
LB1/2	LB1	M_1	L	VII	59	6	9.0	(9.6)	10.4	*(7.9)*	*9.1*	*12.5, 12.4*[e]
LB6/1	LB6/1	M_1	R	XI	51	5[b]	8.8	9.1	10.0	—	—	—
LB6/1	LB6/1	M_1	L	XI	51	4	9.0	9.3	10.0	—	8.8	—
LB1/2	LB1	M_2	R	VII	59	3.5	9.9	10.1	10.1	*8.6*	*8.8*	*12.5, 11.8*[e]
LB1/2	LB1	M_2	L	VII	59	4	9.7	10.1	10.0	*9.0*	*9.0*	*12.5, 11.7*[e]
LB6/1	LB6/1	M_2	R	XI	51	4	9.5	9.8	9.6	—	—	—
LB6/1	LB6/1	M_2	L	XI	51	3	9.6	9.8	9.5	—	—	—
LB1/2	LB1	M_3	R	VII	59	4	8.9	8.9	9.5	*7.9*	*8.3*	*15.8, 14.5*[e]
LB1/2	LB1	M_3	L	VII	59	3	9.8	9.8	9.6	*8.5*	*8.2*	*15.1, 14.0*[e]
LB6/1	LB6/1	M_3	R	XI	51	3	8.9	9.0	8.8	—	—	—
LB6/1	LB6/1	M_3	L	XI	51	3	8.9	8.9	8.5	—	—	—

[a] Measurements based on CT are in italics.
[b] Revised from Jungers and Kaifu et al. (2011).
[c] Estimated original crown diameter allowing for wear.
[d] Lengths for mesiobuccal, distobuccal, and lingual roots, respectively.
[e] Lengths for mesial and distal roots, respectively.

Figure 4. LB8/2, a right mandibular second premolar, was recovered by wet-sieving from spit 61 of sector VII (Morwood and Jungers, 2009). This tooth is unique, showing exceptionally good preservation with transparent texture, among the bone remains from the Pleistocene levels of Liang Bua, and is likely a contamination from the upper stratigraphic level. Therefore, we exclude this specimen from our *H. floresiensis* dental sample.

Methods

Tooth crown measurements follow the methods described in Wood (1991). Both the measured and wear-corrected

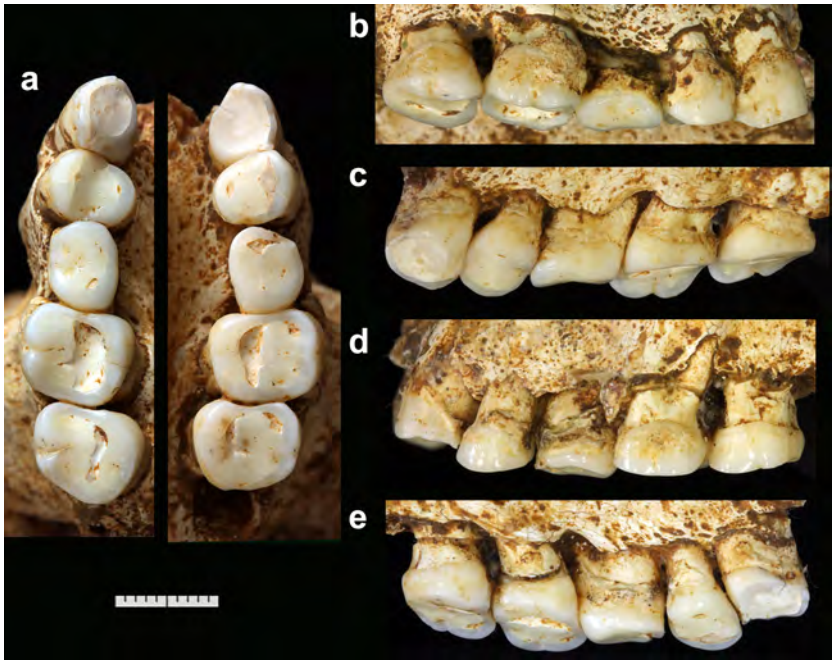

Figure 1. Maxillary dentition of LB1. Occlusal views (a). Buccal (b) and lingual (c) views of the right dentition. Buccal (d) and lingual (e) views of the left dentition. Micro-CT scan indicates that right M^3 was congenitally absent in this individual. Note that both right and left P^4s are rotated bilaterally. Scale = 10 mm.

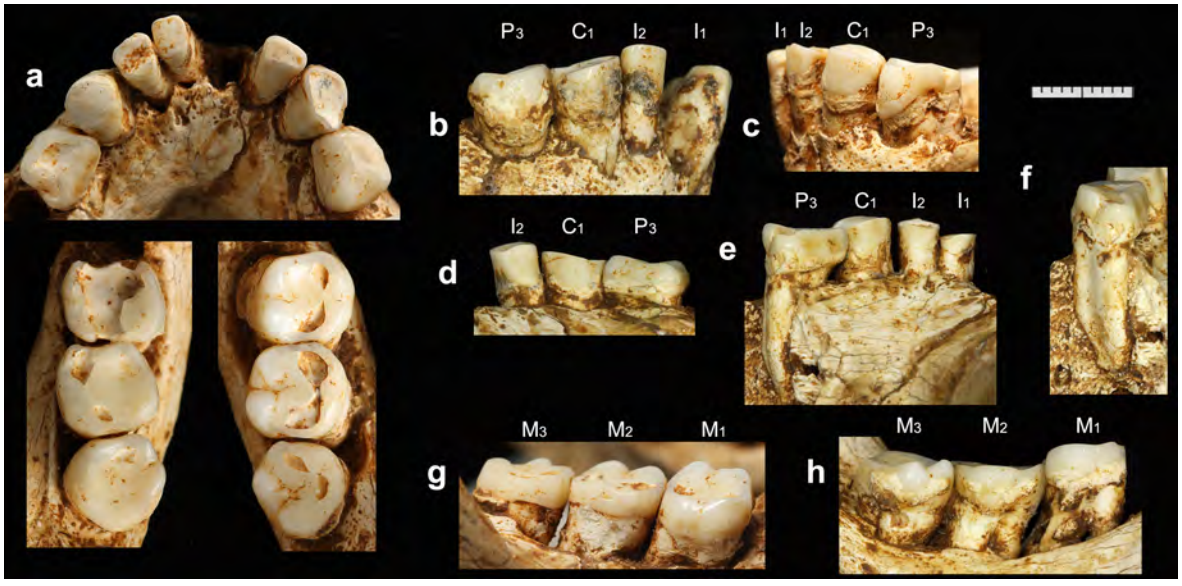

Figure 2. Mandibular dentition of LB1. Occlusal views (a). Buccal views of the anterior parts of the right (b) and left (c) dentitions. Lingual views of the anterior parts of the right (d) and left (e) dentitions. Distal view of the left P_3 root (f). Buccal view of the right molars (g). Lingual view of the left molars (h). (e) and (f) were taken when we disassembled the left mandibular body to correct its reconstruction. Scale = 10 mm.

values are reported for mesiodistal (MD) crown diameters. Length of a root was measured on the buccal surface (from the cervical midpoint to the root tip) except for the lingual root of the upper molar where the length was taken on the lingual surface. A single observer (Y.K.) measured the original specimens with reference to isolated plaster casts of each tooth, using a Mitsutoyo digital sliding caliper with pointed tips. When necessary, the thickness of dental calculus deposit was estimated to obtain the original crown diameters. Cervical diameters were measured either by a sliding caliper (by Y.K.) or from the CT scan (by R.T.K.) following the methods of Hillson et al. (2005). Severity of occlusal wear was scored by the categories (0–8) proposed by Smith (1984).

High-resolution CT scan was obtained using the microfocal X-ray CT system TX225-ACTIS (Tesco Co.) in April

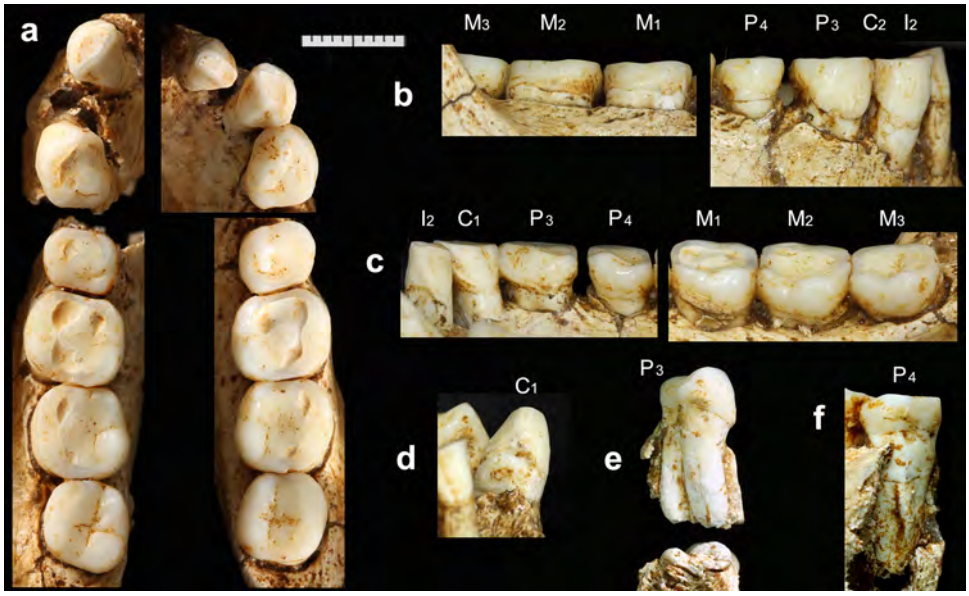

Figure 3. Mandibular dentition of LB6/1. Occlusal views (a). Buccal (b) and lingual (c) views of the right dentition. Mesial view of left C_1 (d). Mesial (upper image) and apical (lower image) views of left P_3 (e). Mesiolingual view of left P_4 (f). (e) and (f) were taken when Y.K. disassembled the left mandibular body for conservation purposes. Scale = 10 mm.

2009 at the University Museum, The University of Tokyo (Kaifu et al., 2011). Prior to the scan, the system was calibrated with known size phantoms. Linear measurement error in a horizontal plane was less than 0.1% (Kubo et al., 2008). Original scans were taken at 130 kV and 0.20 or 0.17 mA with a 0.5 or 1 mm thick copper plate prefilter to lessen beam-hardening effects. Other scanning parameters included a 512 × 512 matrix, 50 or 80 microns pixel size, and 50 or 80 microns slice thickness and interval. Avizo 8.0 software (FEI Visualization Sciences Group) was used for segmentation of the enamel and the dentine to visualize the EDJ surfaces.

Morphological Description

Table 1 reports our measurements of the crowns and roots. These measurements are in most cases slightly lower (0.1–0.9 mm, or more in a few cases) than those reported by Brown et al. (2004) and Brown and Maeda (2009). It should be noted that there is substantial asymmetry in the degree and pattern of occlusal wear in LB1. This is because of the horizontally twisted (rotated) occlusion between the maxillary and mandibular dentitions in this individual, which was probably caused by posterior positional (deformational) plagiocephaly (Kaifu et al., 2009, 2010).

Different individuals exhibit similar dental characters to each other unless noted otherwise. Anatomical terminology mostly follows Johanson et al. (1982). The following abbreviations are used:

MD = mesiodistal(ly)
BL = buccolingual(ly)
LL = labiolingual(ly)
CEJ = cemento–enamel junction
EDJ = enamel–dentine junction
IPF = interproximal facet
Mmr = mesial marginal ridge
Dmr = distal marginal ridge
ASUDAS = Arizona State University Dental Anthropology System (Turner et al., 1991)

Incisors

I^1: LB15/2 (left: Figure 4)

The specimen is complete except for partial exfoliation of the cementum from the root surface and a small damage at the root tip. Extensive occlusal wear has eliminated most of the crown, leaving a flat, slanting occlusal surface that reaches the CEJ on the distal face but not on the mesial face. Mesial and distal IPFs are not present. Small patches of dental calculus are attached around the CEJ.

Viewed occlusally, the preserved cervical portion of the labial enamel surface is nearly straight, suggesting a limited labial MD convexity of the crown when unworn. In mesial or distal view, the labial cervical enamel is flattened so that it continues straight to the root surfaces. The remaining small portion of the lingual enamel suggests that the gingival eminence was weak. The ASUDAS scores for shoveling and tuberculum dentale are not available due to the wear.

At the cervical level, the cross-sectional shape of the root is a MD compressed, rounded triangle with the mesiolingual face slightly wider and more convex than in the distolingual face. The root is short (our estimate of the labial length is 12–13 mm), stocky, and retains its thicknesses for 4 mm above the CEJ before tapering toward the broken tip. This root length is largely comparable to the mean root length (distance between the root apex and the center of the cervical plane) of a recent modern human sample reported by Le Cabec et al. (2013) (12.9 mm).

I^2

This tooth is not represented in the currently available Liang Bua collection. Although Brown et al. (2004) inferred

Figure 4. Four isolated teeth of *H. floresiensis* from Liang Bua: LB 15/2 (left I^1), LB 6/14 (left I_1), LB 2/2 (left P_3), and LB 15/1 (right P_4). From left to right, occlusal (o), mesial (m), labial/buccal (l/b), and distal (d) views. Scale = 10 mm.

that the I^2 was much smaller than I^1 in LB1, this view is not supported by the partially preserved, moderate-sized right I^2 alveolus seen in a CT section (Figure 5a).

I_1: LB1 (left: Figure 2), LB6/14 (left: Figure 4)

The former is complete and is in the alveolus of the LB1 mandible. LB6/14 is an isolated tooth that was not described by Brown and Maeda (2009). It has a slight damage at its root tip. Its size, morphology, wear, and preservation suggest that the tooth is from the LB6/1 mandible, but this possibility cannot be ascertained due to the damage on the latter. Incisal wear is extensive in both specimens. The areas of the CEJ and exposed root surfaces are in part covered by thin layers of dental calculus.

The preserved basal portions of the crowns do not show marked lateral flaring. Viewed mesially or distally, as in the I^1, the labial cervical enamel is flat and continues straight to the labial root surface. A shallow but distinct vertical furrow is present on the labial crown face of each specimen. It reaches and disappears at the CEJ. This may indicate that the crown had assumed double-shoveling when unworn. On the lingual face, the gingival eminence is weak and almost absent.

The root can be examined directly (LB6/14: Figure 4) or with the CT scan (LB1: Figure 6b). The root is MD compressed and has a vertical furrow on the distal face. Viewed mesially or distally, the lingual (LB6/14) or both the labial and lingual (LB1) outlines are markedly convex so that the maximum LL diameter (5.8–6.0 mm), which measures around the middle of the root length, considerably exceeds the LL diameter at the CEJ (5.0 mm). The root lengths, 14 mm (LB1) and 12.2 mm (LB6/14), are largely comparable to the mean values for various modern human samples (11–13.4 mm: Suwa et al., 2011, Table 3).

I_2: LB1 (right and left: Figure 2), LB6/1 (right: Figure 3)

The three specimens are in their alveoli. They are complete except for damages at the root apices of LB1. Wear is moderate (LB1 right, LB6/1) to extensive (LB1 left). The left tooth of LB1 exhibits a 'stepped' occlusal wear in which the lingual half is worn more heavily than the labial half. The CEJs are in part covered by thin layers of calculus.

Basic anatomy is similar to I_1, although I_2 is larger and its labial crown surface faces slightly distally. Viewed labially, the crown is slender MD. On the unworn cervical half of the labial face, a vertical furrow seen in the I_1s does not develop, but the surface is flattened MD. As in the other incisors, the labial enamel and root surfaces continues straight with little swelling of the cervical enamel. On the smooth lingual face, the gingival eminence is weak. Basal parts of the Mmr and Dmr are barely recognizable near the worn incisal margin of LB6/1, although the wear prevents ASUDAS scoring for this trait.

CT scan of LB1 (Figure 6a) indicates that its root form is generally similar to that of the I_1s. The MD compressed root presents a longitudinal groove on the distal face. The labial root face shows marked vertical convexity, and LL diameter reaches its maximum around cervical one-third of the root length. The root length of the LB1 I_2, 14.3 mm, is largely comparable to the mean values for various modern human samples (12–14.7 mm: Suwa et al., 2011, Table 3).

Canines

C^1: LB1 (right and left: Figure 1)

Both teeth are in their sockets. Each of them is complete except for a transverse crack in the middle of the root (visible in the CT scan). Occlusal wear is extensive, leaving only 1–2 mm of the mesial enamels. The right tooth is less worn, particularly on its labial side, so that its occlusal surface is strongly sloping lingually. Mesial IPF is lacking. The crown contacts with the P^3 at the distal aspect of its Dmr. An intermittent band of calculus covers the CEJ or root surface, particularly on the labial side.

The severe wear obscures the labial crown contour, but a low distal shoulder is evident in the less worn right tooth. Viewed occlusally, the crown outline is asymmetric with the convex mesiolabial and flattened distolabial aspects. On the less worn right tooth, a MD broad, rounded gingival

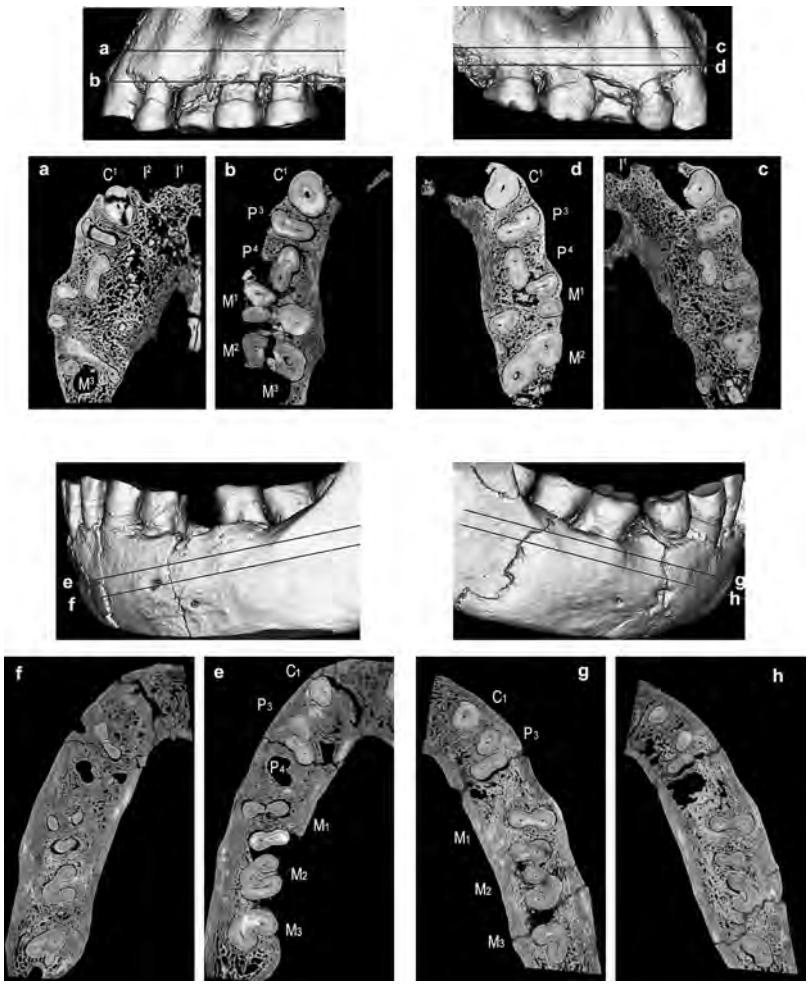

Figure 5. CT sections of the dental roots of LB1. The level for each section is indicated in the image above the relevant section. Upper left (sections a and b): left maxillary dentition. Upper right (sections c and d): right maxillary dentition. Lower left (sections e and f): left mandibular dentition. Lower right (sections g and h): right mandibular dentition.

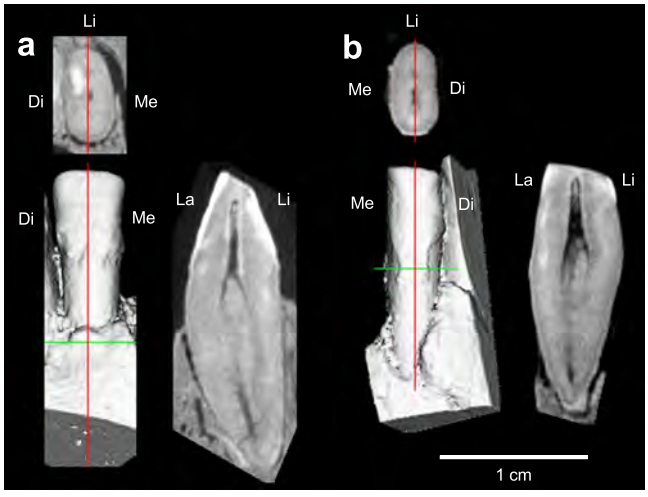

Figure 6. CT sections of the LB1 mandibular incisor roots. Sagittal (top) and horizontal (right) sections are shown for right I_2 (a) and left I_1 (b). The lower left image for each tooth is a surface rendered image of the labial side, which indicates the levels of the sections (vertical and transverse lines). Me = mesial, Di = distal, La = labial, Li = lingual. Note the convex labial and lingual root outlines similar to LB6/14, the isolated I_1 shown in Figure 4.

eminence dominates the lingual aspect. It does not project lingually over the cervical line, but smoothly continues to the prominent basal part of the lingual median ridge. Dmr is a weak, thin line restricted near the crown's distal shoulder. The labial crown face exhibits slight wrinkling.

CT scan indicates that the root is single and robust, with its labial (right tooth) or lingual (left tooth) face showing marked vertical convexity. The cross section is MD compressed, oval with the labial section broader than the lingual (Figure 5a–d). The lengths of the root, 20.3 mm (right) and 19.8 mm (left), are greater than the modern human average (16.1 mm) and are slightly shorter than the means for Neanderthals (22.5 mm) and the Early Pleistocene *H. erectus* from Sangiran, Java (21.5–21.6 mm) (Le Cabec et al., 2013).

C_1: LB1 (right and left: Figure 2), LB6/1 (right and left: Figure 3)

The four specimens from two individuals are complete and in their alveoli. Approximately half (LB6/1) or slightly more (LB1) of the crown heights have been lost by wear that produces largely flat occlusal surfaces. Mesial and distal IPFs are present in the less worn LB6/1 C_1s, but mesial IPFs were probably lost in LB1 by wear.

The distal crown shoulder is preserved on the relatively unworn left C_1 of LB6/1. Its tip is located 3.5 mm above the CEJ, and is distinctly lower than the worn mesial shoulder that measures >5 mm. Apart from this asymmetry, the wear prevents assessment of labial crown contour. Viewed occlusally, the gently convex buccal crown contour is nearly symmetric but the lingual contour is asymmetric due to the distally located gingival eminence. The labial face is characterized by fine, longitudinal wrinkles and a slight thickening of the cervical enamel (evident in the calculus-free cervical enamels of LB6/1: Figure 3b). There are no longitudinal grooves along the mesial and distal aspects of the labial crown surfaces. The lingual face is dominated by a broad, prominent median ridge that continues smoothly from the gingival eminence. Weak lingual Mmr and Dmr are represented by flattened areas beside the median ridge, and the mesial and distal lineal foveae are no more than shallow depressions.

CT scan (Figure 5e, g) indicates that the root is single and relatively robust, with vertically convex lingual face and vertically straight labial face. The root lengths for LB1, 17.2 mm (right) and 16.4 mm (left), are comparable to the mean values for various modern human samples (13.7–18.2 mm: Suwa et al., 2011, Table 3).

Premolars

P^3: LB1 (right and left: Figure 1)

The specimens are complete except for a crack at the root of the left tooth, which has dislocated its crown slightly mesially and occlusally. The left tooth is worn flat with dentine islands of moderate sizes exposed on the two cusps. On the less worn right tooth, the lingual cusp (protocone) is worn flat whereas the buccal cusp (paracone) remains high. Mesial and distal IPFs are present, although the left tooth has lost its contact with the P^4 due to the dislocation. A thin layer of calculus covers the cervical half of the buccal crown surface of the right tooth. Calculus is present, but less marked on its lingual face and on the left tooth.

The occlusal outline, partially obscured by the interproximal wear, is ovoid with MD diameters slightly greater across the buccal than the lingual crown. The crown is largely symmetrical MD, with the lingual cusp tip shifted slightly mesially. Detailed morphology of accessory occlusal ridges is unknown due to the wear, but some features are evident. The longitudinal groove is completely worn away, whereas the anterior and posterior fovea partially remain unworn. On the EDJ surface, there is a sharp crest that connects the two cusps (Figure 7a), indicating the presence of a well-developed transverse crest when the crown was unworn. The low Mmr and Dmr are incised by grooves emanating from the mesial and distal foveae, respectively. On the relatively vertical and smooth buccal face, the area around the CEJ is obscured by the calculus deposition, but the presence of a narrow enamel band along the cervical line is evident on the left tooth. Mesial and distal buccal grooves are absent although the area of the former is flattened in the left tooth. The lingual face is also smooth and steep.

CT scan (Figure 5a–d) indicates that the root has a buccal component and a lingual component that are extensively fused together to form a BL broad, plate-like root complex. The buccal component is longer than the lingual one. Each component has its own, single root canal in the right tooth, whereas the canals are partially connected to each other in the left tooth. A vertical furrow intervenes between the two components on the mesial and distal root faces. The furrow is deeper on the mesial than on the distal faces, and is more marked on the right tooth.

P^4: LB1 (right and left: Figure 1).

The right tooth is complete. In the left tooth, enamel is chipped off from the distobuccal corner of the crown, and the root is cracked so that the crown is dislocated slightly occlusally. Both teeth are rotated ~90° and their original buccal faces orient mesially in the tooth rows. Occlusal wear is heavier on the left than on the right tooth. Both teeth contact with their mesial and distal adjacent teeth, although the mesial side of the left tooth presently lacks the contact due to the postmortem mesial dislocation of the P^3. Calculus deposition is marked on the buccal but much less on the lingual sides.

The occlusal outline, partially obscured by wear, is elliptical with nearly equal paracone and protocone cusp breadths. The protocone cusp tip is located slightly mesially to the crown's midline (lingually in the dentition because of the rotation). The worn occlusal enamel surface of the left tooth is featureless except for a dentine exposure at the paracone tip. On the less worn right tooth, the mesial half of the longitudinal groove has been worn away but its distal half as well as the anterior and posterior foveae remain intact at least partially. On the EDJ surface, there is a sharp crest that connects the two cusps (Figure 7b), indicating that a well-developed transverse crest was present when the crown was

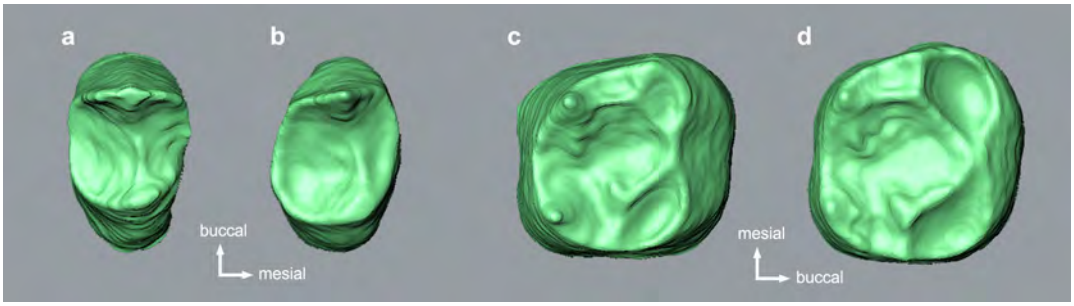

Figure 7. Occlusal views of the EDJ surfaces of the right P^3 (a), P^4 (b), M_1 (c), and M_2 (d).

unworn. A short accessary ridge extends from the paracone cusp tip toward the posterior fovea. The low, incomplete Dmr remain unworn, whereas the Mmr is obliterated except for its buccal (mesial in the tooth row) segment. Both the buccal and lingual faces rise steeply from the CEJ. Mesial and distal buccal grooves are absent on the less worn right tooth.

CT scan (Figure 5a–d) indicates that the root is largely similar to those of the P^3s. The buccal and lingual components of similar lengths are extensively fused to form a BL broad, plate-like root complex. A longitudinal furrow separating the two components is deeper on the mesial face than on the distal face.

P_3: LB1 (right and left: Figure 2), LB2/2 (left: Figure 4), LB6/1 (right and left: Figure 3)

LB2/2 is an isolated tooth. The other four teeth are in their sockets. All the five specimens are complete. Flatly or concavely worn occlusal surfaces are slightly (LB1, LB6/1) to strongly (LB2/2) beveled distally. Moderate occlusal wear exposes a large dentine island on the buccal cusp of each specimen. In the tooth row, the P_3s of LB1 are slightly rotated so that their mesiobuccal surfaces contact with the canines, whereas the LB6/1 P_3s contact with the canines at their pointed mesial end of the mesial occlusal ridge (thus these P_3s are not rotated, in contrast to the condition in LB1). Mesial and distal IPFs are also present in the isolated LB2/2, but the former is located on the mesiobuccal surface, indicating a slight rotation as in LB1. The buccal and lingual faces of these teeth are variably covered by dental calculus with the most severe cases observed in LB1.

Viewed occlusally with the mesial and distal protoconid (buccal cusp) ridge oriented transversely, the crown is a distorted fan composed of a gently (LB1, 6/1) or moderately (LB2/2) convex and MD long buccal aspect and distally tapering lingual crown. It is extensive both MD and BL, although the MD diameter for LB1 reported by Brown and Maeda (2009), 10.4 mm, is an overestimate irrespective of crown orientation. The prominent buccal cusp supports MD extensive mesial and distal protoconid ridges (evident from the preserved enamel and thick lines of exposed dentine). The lingual cusp (metaconid) is small and is situated distally, shortly mesial to (LB6/1) the crown's distolingual corner. The two cusps are connected by a strong transverse crest that runs diagonally toward the crown's distolingual section, almost in line with the cervical long axis. Mesial to this crest and lingual to the mesial protoconid ridge, the entire mesiolingual segment of the occlusal surface slants and faces mesiolingually to form an extensive, sloping, generally flat but finely wrinkled enamel surface. This beveled surface extends inferiorly to the level ~1 mm short of the CEJ. The short, poorly developed Mmr and the shallow, linear anterior fovea are restricted to the mesial aspect of this sloping surface. On the distal crown, the talonid is represented by a low, featureless Dmr that is restricted to the distal crown margin and delimits a BL oriented, linear posterior fovea. The buccal face slopes lingually and curves moderately (LB1, LB6/1) or strongly (LB2/2) in a vertical section. There are no distinct mesial/distal buccal grooves, but the entire buccal face is irregularly wrinkled. A 1 mm wide band of enamel develops along the cervical line on the buccal face of LB1 (evident on the calculus-free left side: Figure 2c). The buccal cervical line dips inferiorly so that the crown is deeper on the buccal than on the lingual aspect.

Based on low-resolution CT scans, Brown and Maeda (2009) described that LB1 and LB6/1 had two roots arranged in a 'MB + D' pattern (a circular mesiobuccal root and a larger plate-like distal root) defined by Wood et al. (1988), and the isolated LB2/2 a Tomes' root with a deep mesiolingual cleft resulting from fusion of the original mesiobuccal and distal components. Our high-resolution CT scan and direct observation (Figure 2f) of LB1 as well as direct observations of LB6/1 (Figure 3e) and LB2/2 (Figure 4) confirm these assessments. The two root components of LB1 and LB6/1 are closely set to each other, particularly in their apical portions (Figure 3e (lower), Figure 5f, h). The cervical outline of the *H. floresiensis* P_3 root is elliptical with its long axis being almost in line with the transverse crest on the crown. The root lengths (10.7–13.5 mm: Table 1) are shorter compared to the mean values for various modern human samples (12.7–17.0 mm: Suwa et al., 2011, Table 3).

P_4: LB6/1 (right and left: Figure 3), LB15/1 (right: Figure 4)

LB15/1 is an isolated tooth that was not described by Brown and Maeda (2009). The LB6/1 P_4 are in their alveoli, although the mesial root of the left tooth is now visible at the break of the mandible. The three specimens are complete. Occlusal wear is moderate, and the less worn LB6/1 right tooth still retains some cuspal relief. All three teeth have mesial and distal IPFs that reach the occlusal surfaces. Small patches of calculus remain on the CEJ and enamel surfaces.

The crown of LB15/1 is larger than LB6/1, and is probably so compared to LB1 where the space between its left P_3 and M_1 measures <7 mm. The occlusal contour is asymmetric with slightly protruding mesiobuccal and distolingual corners. The buccal and lingual cusps are located mesially, and are connected by a well-developed transverse crest (evident in LB6/1 and may be so in the worn LB15/1). The Mmr is incised by a shallow groove emanating from the anterior fovea (observable only in the right tooth of LB6/1). The talonid basin is large, situated at a low level, and supports a linear distal fovea and a thick Dmr. The Dmr continues to the crown's distolingual corner, smoothly flexes mesially to extend toward the lingual cusp tip. Mesial and distal buccal grooves are absent on the smoothly convex buccal crown face. The lingual face is unremarkable.

The remaining alveolus for the LB1 left P_4 (Figure 5f, e) and mesial aspect of the LB6/1 left P_4 (Figure 3f) indicate that these two teeth are categorized as Tomes' root with a deep mesiolingual cleft. The partial fusion of the LB6/1 root is not clearly recognized in Figure 13 of Brown and Maeda (2009) who erroneously reported that this tooth shows MB + D root pattern. The isolated LB15/1 has a single, robust root (Figure 4). Its MD diameter is greatest at the cervix (5.9 mm) and tapers toward the apex, whereas the large BL diameter remains almost the same in its cervical half (7.7–7.2 mm). A shallow vertical groove is present on the distal root face, but the mesial face is generally convex. The root lengths (13.2–14.3 mm: Table 1) are comparatively shorter than the mean values for various modern human samples (12.9–16.5 mm: Suwa et al., 2011, Table 3).

Molars

M^1: LB1 (right and left: Figure 1)

The specimens are complete except for cracks at the root of the left tooth. The lingual half of the occlusal surface is severely worn, resulted in the exposure of a MD continuous, concave dentine surface in a form of 'cupped wear.' The buccal half is less worn particularly in the right tooth. BL extensive mesial and distal IPFs are present. The enamel surface and CEJ are partially covered by thin calculus deposits, particularly on the buccal face of the right tooth.

The occlusal contour is a BL elongated square with a wider mesial segment that results from lingual projection of the protocone base. The wear has eliminated most of the occlusal ridge and groove structures, but the remaining grooves indicate that both the right and left teeth had four major cusps. On the right tooth, much of the buccal transverse occlusal groove remain. On the left tooth, the same groove can be traced only by an indentation on the buccal occlusal margin and two tiny, shallow pits near the crown midpoint, the lingual one of which probably corresponds to the central fovea. Near the distal occlusal margin and lingual to a tiny dentine exposure at the metacone apex, a small pit and a short groove remain. The latter is probably a part of the groove demarcating the metacone and hypocone. The prominent distolingual corner of the crown suggest strong development of the hypocone (ASUDAS grade 4 or 5). The buccal face is obscured by the calculus but the presence of a 0.5 mm wide enamel band is evident along the cervical enamel. The smooth lingual crown face is marked by a lingual projection of the protocone base, but no expression for the Carabelli's trait.

CT scan (Figure 5a–d) indicates that the mesiobuccal, distobuccal, and lingual roots are divergent from each other. The lingual face of the lingual faces distolingually (Figure 1a). The above described lingual swelling of the protocone base is apparently associated with this 'twisted' root orientation.

M^2: LB1 (right and left: Figure 1)

The crown on the left side is dislocated slightly buccally at a large crack on its root. A small crack is also present in the distobuccal root of the right tooth. Otherwise, the two specimens are complete. The occlusal surface is worn flat with dentine exposed at two cusps on the right (protocone and hypocone) and left (protocone and paracone) teeth. Distal IPF is present only on the left tooth. It measures 2.2 mm both BL and vertically. A few thin or small patches of calculus remain mainly on the buccal crown face of the right tooth.

These are four-cusped teeth. The occlusal outline is a trapezoid with broader mesial section as well as distally extended hypocone but reduced metacone, which is more marked in the right tooth. Much of the occlusal enamel structures have been lost by wear. The buccal transverse occlusal groove, which runs lingually and mesially, is clearly (right) or partially (left) recognizable. The central fovea is represented by a shallow pit near the center of the left tooth, but no such feature remains on the right tooth. Other occlusal groove/ridge structures are not evident, although our CT-based examination of the EDJ topology indicates that tiny pits on the lingual aspect of the right tooth represent the lingual transverse occlusal groove. A 0.5 mm enamel band is present along the cervical line of the buccal face. Although the lingual face shows marked lingual projection mesially as mentioned above, the entire surface is smooth and Carabelli's feature is absent.

CT scan (LB1 only: Figure 5a–d) indicates that the root structure is largely similar to the M^1s. There are three roots (mesiobuccal, distobuccal, and lingual) and the lingual root exhibits distal twisting. However, compared to the M^1 condition, these roots are less divergent, the level of split of the three roots is more apical, and the mesiobuccal and lingual roots are fused extensively in the left tooth.

M^3

Morphology of this tooth can be inferred only from the left alveolus of LB1 (Figure 5a). Its small, conical form suggests that this tooth had a much smaller crown than M^1 and M^2 (Brown et al., 2004).

M_1: LB1 (right and left: Figure 2), LB6/1 (right and left: Figure 3)

These teeth are in their sockets. Small portions of enamel have been chipped off at the mesiolingual and distobuccal corners of the left tooth of LB1 either before or after the individual's death. Otherwise, the four specimens are complete. Mesial and distal IPFs are present in all of the teeth. Asymmetric wear pattern in LB1 (less worn lingual cusps of the right tooth, loss of mesial and distal enamels in the left tooth, etc.) is primarily because of the unbalanced, rotated occlusion in this individual (Kaifu et al., 2009). Calculus depositions are seen around the buccal and lingual CEJs. It is extremely thick and extensive on the lingual face of the right tooth of LB1. A filled hole on the buccal face of the mesial root of the LB6/1 right tooth was made to take samples for DNA extraction.

The occlusal contour is a MD short, rounded square with slightly protruding mesiobuccal and distolingual corners. Much of the enamel surface structures have been worn away, but the partially remaining occlusal grooves, the arrangements of the exposed dentine patches, as well as the EDJ surface (Figure 7c, LB1 only) indicate that these are four-cusped teeth with no development of hypoconulid, Cusp 6, and Cusp 7. The lingual transverse occlusal groove, parts of the buccal transverse occlusal groove, and the mesial portion of the distal longitudinal groove (LB6/1 only) are traceable. A mesiobuccally oriented, short groove at the central fovea (evident on the right tooth of LB1 and possibly both teeth of LB6/1) suggest a substantial contact relationship between the metaconid and hypoconid. Entoconid is the lingually restricted, smallest cusp. Metaconid is also restricted BL, and the two buccal cusps dominate on the occlusal surface. At the buccal termination of the transverse lingual occlusal groove, the central fovea is shallow with no development of a deep pit. A sharp, high, and continuous crest connecting the protoconid and metaconid on the EDJ surface of LB1 (Figure 7c), which corresponds to grade 3 of Bailey et al. (2011: Fig. 4), strongly suggests the presence of a mid-trigonid crest before the wear (Bailey et al., 2011; Martínez de Pinillos et al., 2014; the definition of 'mid-trigonid crest' follows Martínez

de Pinillos et al., 2014). A protostylid is absent in the LB1 right M_1, and at least not evident on the moderately worn other M_1s. There is a faint, narrow band (LB1) or swelling (LB6/1) of enamel along the cervical lines.

CT scan (LB1 only: Figure 5e–h) indicates that M_1 has plate-like mesial and distal roots that are distinctly separated from each other. The BL broad mesial root is bifid apically. The BL width of the distal root decreases apically. The mesial root lengths of LB1 (12.3–12.5 mm: Table 1) are shorter than the mean values for various modern human samples (13.2–14.9 mm: Suwa et al., 2011, Table 3).

M_2: LB1 (right and left: Figure 2), LB6/1 (right and left: Figure 3)

The four specimens are complete. The lingual cusps are variably less worn and the original cuspal reliefs and groove patterns can be read to some extent. Mesial and distal IPFs are present, and some amounts of calculus deposition are seen, particularly on the lingual faces. A filled hole on the buccal face of the mesial root of the LB1 right M_2 was made to take samples for DNA extraction.

The occlusal outline is a rounded square with slight mesial projection of the protoconid and lingual projection of the entoconid base. These are four-cusped teeth. Two occlusal grooves demarcating the entoconid are preserved. Much of the other occlusal grooves have been worn away, but their positions can be restricted with reference to the anterior fovea (LB6/1), distribution of the exposed dentine for the protoconid and hypoconid (LB1 and LB6/1), the remaining groove between the metaconid and hypoconid (LB1), and the topology of EDJ seen in the CT scan (LB1). Cusp arrangement is similar to the M_1s: Entoconid is the lingually restricted, smallest cusp. Metaconid expands slightly more buccally than the entoconid, but the two buccal cusps are more expansive BL on the occlusal surface. Metaconid and hypoconid contact to each other via a short occlusal groove in LB1, and this seems to be also the case for LB6/1. Cusp 7 assumes a form of a triangular depressed area immediately distal to the main occlusal ridge of the metaconid in LB1, whereas this structure is not clearly developed in LB6/1. The anterior fovea, evident in LB6/1, is a small, triangular notch that opens mesially. A sharp, high, and continuous crest connecting the protoconid and metaconid on the EDJ surface of LB1 (Figure 7d), which corresponds to grade 3 of Bailey et al. (2011: Fig. 4), strongly suggests the presence of a mid-trigonid crest before the wear (Bailey et al., 2011; Martínez de Pinillos et al., 2014). No deep pit develops at the central fovea as in the M_1s. The distal longitudinal groove disappears before reaching the distal occlusal margin without forming a distinct posterior fovea. The buccal crown face is generally smooth except for a narrow, continuous enamel band stretching along the cervical line over the protoconid and hypoconid bases. The lingual face is vertically more convex compared to the M_1 condition.

CT scan (LB1 only: Figure 5e–h) indicates that the mesial and distal root components are fused along their buccal sides to form a short, cylindrical root complex with a C-shaped cross section. The mesial root length of LB1 (12.5 mm) is shorter than the mean values for various modern human samples (13.1–15.1 mm: Suwa et al., 2011, Table 3).

M_3: LB1 (right and left: Figure 2), LB6/1 (right and left: Figure 3).

The four specimens are complete except for minor cracks at the root of the LB1 right tooth. The teeth contact with the M_2s, although the LB1 M_3s are bilaterally rotated ~30° so that their mesial faces orient lingually. A filled hole on the lingual root face of the LB1 left tooth was made to take sample for DNA extraction.

The occlusal contour is a rounded rectangle with the lingually protruded entoconid (LB6/1) or a pear-shape with the broader distal crown (LB1). These are four-cusped teeth. The occlusal groove arrangement is close to a '+' pattern although metaconid and entoconid slightly contact each other. The longitudinal groove and the transverse groove are situated lingually and distally relative to the crown center, respectively, so that protoconid is the largest cusp. The mesial segment of the longitudinal groove incises the Mmr, whereas its distal segment does not reach the distal occlusal margin. The anterior fovea is a triangular pit opening mesially. The central fovea is not very deep, and there is no posterior fovea. Cusp 7 is defined as a triangular depressed area distal to the main occlusal ridge of the metaconid. A thin enamel band is expressed along the cervical line on the buccal crown face of LB1, whereas the same face is generally smooth in LB6/1. The lingual crown face is vertically more convex than in the anterior molars.

CT scan (LB1 only: Figure 5e–h) indicates that the M_3 of LB1 has a single, pyramidal, long root with a deep buccal cleft. The mesial root lengths of LB1 (15.8 and 15.1 mm) are greater than the mean values for various modern human samples (11.2–14.4 mm: Suwa et al., 2011, Table 3).

Dentition and occlusion

LB1

LB1 had a completed permanent dentition, but had lost all the maxillary incisors, left M^3, right I_1, and left P_4 postmortem (Brown et al., 2004). Brown and Maeda (2009) reported that their CT scans suggested the presence of a very small M^3 odontome within the alveolar bone of the LB1 maxilla. Our micro-CT scan identifies no such evidence (the white materials behind the M^2 in Figure 5a–d are probably dirt), indicating that this tooth was congenitally absent as reported originally (Brown et al., 2004). Brown and Maeda (2009) also inferred that the right P_4 was originally present in the jaw, but the right P_3 bears no distal IPF and a remnant of the P_4 or its alveolus is not observed in our CT scan (Figure 5g, h). We suggest that the right P_4 was congenitally absent and a single, BL elongated (4.1 mm wide) mesial IPF on the M_1 was a facet for the exfoliated dm_2 (Kaifu et al., 2009). The space between the right P_3 and M_1 has been reduced to 1.8 mm by mesial migration of the latter.

The maxillary dental arcade shape is described as nearly square with sharp flexion at the canines as seen in *H. habilis*, *H. ergaster*, and Sangiran *H. erectus*, but is different from the more rounded arcades seen in Kabwe and Zhoukoudian 13 (Kaifu et al., 2011). The close proximity between the right I^2 and C^1 alveoli evident in a CT section (Figure 5a) does not support the previous inference for a diastema in this individual (Brown et al., 2004). At variance with the previous report (Brown and Maeda, 2009), the Curve of Spee is

not strong but weak after the correction of the original left row (Kaifu et al., 2009). Bilateral rotations are seen in the P^4s (markedly), M_3s (moderately), and P_3s (slightly).

Kaifu et al. (2009) made a photographic reconstruction of the centric occlusion of LB1 primarily by matching the occlusal wear facets. The result indicated that the occlusion of this individual was horizontally twisted so that the left molars show a Class II relationship (the mandibular teeth are in a distal relationship with their normal maxillary opponents) and the right molars a Class III relationship (the mandibular teeth are in a mesial relationship with their normal maxillary opponents) (see their Fig. 2). This distorted occlusion is likely a result of the posterior deformational (positional) plagiocephaly, and is not indicative of severe developmental abnormality in this individual (Kaifu et al., 2009, 2010).

LB6/1

LB6/1 had a complete set of the permanent mandibular dentition, but the right and left I_1 as well as left I_2 were absent in their alveoli when the specimen was recovered. The length–breadth ratio of the dental arcade is similar to that of LB1 before it had been broken (Kaifu et al., 2011). The Curve of Spee is only slight (Brown and Maeda, 2009). No remarkable tooth rotation is observed. The occlusal wear pattern in this specimen indicates occlusion with undistorted, normal Class I relationship.

LB2/2

This individual is represented by a single P_3. As mentioned above, the position of its mesial IPF suggests a slight rotation in the tooth row, as in LB1.

Oral health

There is heavy (LB1) or modest (LB6/1) calculus deposition, and the bone is resorbed in the molar regions of LB1 as described and illustrated previously (Brown and Maeda, 2009; Jungers and Kaifu, 2011). The other four isolated dental specimens (LB2/2, 6/14, 15/1, and 15/2) also exhibit some degree of calculus deposition, suggesting its commonality in *H. floresiensis* from the Liang Bua Cave. The heavy calculus and alveolar resorption in LB1 were probably resulted from the unbalanced, twisted (horizontally rotated) occlusion in this individual. Dental caries is not observed in any of the materials described here. No hypoplastic pits or bands are present on the enamel surfaces. Periapical abscess cavities are also absent in LB1 (maxilla and mandible) and LB6/1 (mandible). Previous claims that the oral health condition of LB1 suggests its agricultural subsistence (thus the individual is from a *H. sapiens* individual: Henneberg and Schofield, 2008) has been rejected by Jungers and Kaifu (2011).

Discussion

Dental individuals

Probably five but possibly four or six individuals are represented in the current dental sample of *H. floresiensis*. These are LB1 (skeleton), LB6/1 (mandible) + 6/14 (I_1), and individuals represented by the other three teeth: LB2/2 (P_3), LB15/1 (P_4), and LB15/2 (I^1). Occlusal wear of the latter teeth varies from severe (LB15/2), moderate (LB15/1), to relatively light (LB2/2). At least, the wear state of LB2/2 does not match with either of the other two teeth, and these three teeth include two or more individuals. In terms of the P_4 crown and root size (Table 1; see above), LB15/1 may have been the largest individual, followed by LB1 and LB2/2 whose P_3 crown sizes are nearly equal to each other. LB6/1 is smaller than LB1 in premolar and molar crown sizes.

Reassessment of the previous evaluations: modern or primitive?

Previous studies have proposed several potentially taxonomically diagnostic dental characteristics of *H. floresiensis*. These are summarized and discussed below.

I^2/C diastema

I^2/C diastema is frequently observed in *Au. afarensis* but is rare in *Au. africanus*, *Paranthropus*, and *Homo* (White et al., 1981; Kimbel and Delezene, 2009). Brown et al. (2004) described that, in LB1, "(s)ize, spacing and angulation of the maxillary incisor alveoli, and absence of a mesial facet on the canines suggest that incisor I^2 was much smaller than I^1, and there may have been a diastema." This inference is not supported by our CT scan, which shows close proximity between the I^2 and C^1 alveoli (Figure 5a).

Canine size

Brown and Maeda (2009) reported that the mandibular canine size of LB1 and LB6/1 is 'small' like various other groups of post-1.7 Ma *Homo*, whereas those of earlier *Homo* and *Australopithecus* were either 'variable,' 'medium,' or 'large' (their Table 3). We here metrically reexamine this claim. Table 2 compares 'relative canine size' among various archaic *Homo* groups and a global sample of modern humans (*H. sapiens*). The 'relative canine size' is defined as dimensional proportion of C_1 (LL diameter) relative to the premolar and molar lengths (additive MD diameters for $P_3 - M_2$ or $P_3 + M_1 + M_2$). The available small fossil sample indicates that relative canine size tends to be smaller in *H. habilis* than in later *Homo*, contrary to the claim of Brown and Maeda (2009). The values for the two *H. floresiensis* individuals are within the upper range of the variation for *H. habilis*, and are also well within the variations exhibited by the later archaic and recent *Homo* groups. Therefore, relative canine size is of limited use to assess the taxonomic affinities of *H. floresiensis*.

P^4 rotation

The P^4s of LB1 are bilaterally rotated parallel to the tooth row. This was cited as a unique trait (Brown et al., 2004) or indicative of some developmental abnormality (Hershkovitz et al., 2007) and/or affinity with local, living 'pygmy' groups of Flores (Jacob et al., 2006). However, tooth rotation is a relatively commonly observed dental anomaly both in modern (Jacob et al., 2006; Lukacs et al., 2006) and pre-modern (e.g. Early Pleistocene *Homo* from Dmanisi (Rightmire et al., 2006) and Konso (Suwa et al., 2007)) hominins as well as other mammals (Natsume et al., 2006), with suggested etiologies including some genetic mechanism and a lack of

Table 2. Dimensional proportion of the mandibular canine and first premolar relative to the postcanine tooth row (%)[a]

	C_1 (LL)		P_3 (MD)	
	$P_3 + P_4 + M_1 + M_2$ (MD)	$P_3 + M_1 + M_2$ (MD)	$P_3 + P_4 + M_1 + M_2$ (MD)	$P_3 + M_1 + M_2$ (MD)
H. floresiensis				
LB1		26.2		30.3
LB6/1	19.7	24.6	24.2	30.1
H. habilis (East Africa, 2.0–1.6 Ma)				
Omo75-14			20.2	25.5
KNM-ER 1802			20.1	25.7
KNM-ER 60000	18.6	23.2	20.1	25.0
OH 7	20.9	26.6	19.0	24.2
OH 13	17.0	21.4	20.5	25.7
OH 16	19.8	24.8	20.9	26.1
H. habilis (mean)	**19.1**	**24.0**	**20.1**	**25.4**
Dmanisi *Homo* (Georgia, 1.75 Ma)				
D211	19.6	24.2	21.0	26.0
D2735	21.5	26.1	22.0	26.7
H. ergaster (East Africa, 1.5–1.0 Ma)				
KNM-ER 992	20.4	25.6	21.7	27.1
KNM-WT 15000	21.7	27.4	20.9	26.4
OH 22			22.2	27.7
Early Javanese *H. erectus* (Sangiran, >1.0 Ma)				
Sangiran 22	21.2	26.6	20.6	25.9
European terminal Early Pleistocene *Homo* (Gran Drina, 0.8 Ma)				
ATD H1	23.4	29.0	20.6	25.5
ATD 6-96			20.8	26.0
African early Middle Pleistocene *Homo* (Tighenif and Baringo, 0.8–0.5 Ma)				
Tighenif 1			19.7	24.4
Tighenif 2			19.0	23.7
Tighenif 3	24.7	30.5	21.1	26.0
KNM-BK 8518			21.2	26.5
Chinese Middle Pleistocene *H. erectus* (Zhoukoudian, 0.75 Ma)				
Zhoukoudian B1		24.5		26.3
Zhoukoudian G1	23.3	29.0	20.9	26.0
Zhoukoudian K1	21.1	26.3	22.2	27.7
Post-*habilis* archaic *Homo* (mean)	**21.9**	**26.9**	**21.0**	**26.1**
H. sapiens (mean)	**20.7**	**25.7**	**19.6**	**24.3**
(N: range)	125: 17.3–24.7	136: 21.6–31.0	167: 17.5–21.9	188: 21.5–27.3

[a] Measurements for the comparative fossil sample were taken by Y.K. based on high-quality casts produced from the original specimens by Y.K. or Gen Suwa except for KNM-ER 60000 (Leakey et al., 2012), Dmanisi (Martinón-Torres et al., 2008), KNM-WT 15000 (Brown and Walker, 1993), Gran Drina (Bermúdez de Castro et al., 1999; Carbonell et al., 2005), Tighenif (Bermúdez de Castro et al., 2007), and Zhoukoudian (Weidenreich, 1937). The *H. sapiens* is a global sample from Asia, Oceania, Europe, and Africa, and is based on high-quality casts prepared by Y.K.

space for the normal tooth eruption (Baccetti, 1998; Natsume et al., 2006). Therefore this trait is not taxonomically diagnostic and does not necessarily indicate a severe growth abnormality.

P_3 crown

The P_3s of *H. floresiensis* are unique and were a focus of attention in previous studies (Brown et al., 2004; Brown and Maeda, 2009). A previous claim that (some of) these are deciduous first molars (Obendorf et al., 2008) has been effectively rejected by Brown (2012) based on crown and root morphology as well as the state of wear. Brown and Maeda (2009) suggested that its MD elongated, asymmetric crown shape represents a (very) primitive hominin condition, which changes to a more derived, molarized, bicuspid, and symmetrical P_3 in later australopiths and early members of *Homo*. According to these authors, the P_3 crown morphology of *H. floresiensis* is also similar to ~1.75 Ma *Homo* from Dmanisi (Martinón-Torres et al., 2008), but metrically distinguishable from *H. erects (sensu lato)* and *H. sapiens* (their Figure 12). Jacob et al. (2006) claimed that the "enlarged, block-like" P_3 similar to the condition in LB1 are observed worldwide in *H. sapiens*, although no numerical data were provided to support their view.

In Figure 8, we compare our revised P_3 crown diameters of *H. floresiensis* with those of a global *H. sapiens* sample as well as the Early Pleistocene *Homo* specimens from East Africa (*H. habilis* and *H. ergaster*), Caucasus (Dmanisi *Homo*), and Java (early Javanese *H. erectus* from the lower and upper stratigraphic levels of Sangiran). In this chart, the P_3s from three *H. floresiensis* individuals are situated at the margin of the large cloud of *H. sapiens* due to the formers' relatively larger MD diameters. MD elongated P_3 crown configurations are frequently observed in *H. habilis* and Dmanisi *Homo*, and represent a primitive state for *Homo* (Wood and Uytterschaut, 1988; Tobias, 1991; Brown and Maeda, 2009). However, contrary to Brown and Maeda (2009), this crown shape is not restricted to *H. habilis* and Dmanisi *Homo* but is also seen in an East Africa specimen dated to 0.8–1.2 Ma (OH 22: Rightmire, 1980; Antón, 2003). Therefore, *H. floresiensis* exhibits a primitive, MD elongated P_3 crown shape shared with *H. habilis*, but such crown morphology does exist, albeit in small numbers, in later *Homo* groups.

P_3 of *H. floresiensis* has a transverse crest that is oriented distolingually, and, at its end, has a small lingual cusp that is situated near the crown's distolingual corner. A similar crest and cusp arrangement, which contributes to reduce the talonid, is found in D2735 from Dmanisi (Martinón-Torres et al., 2008) and a few post-*habilis* African *Homo* P_3s (KNM-ER 992, KNM-WT 15000 (left), OH 22). Although a distally oriented transverse crest is a plesiomorphic hominin condition seen in great apes, *Ardipithecus ramidus*, and *Australopithecus anamensis* (Ward et al., 2001, 2013; Suwa et al., 2009; Delezene and Kimbel, 2011), the P_3s of *Au. afarensis* and *H. habilis* have altered so that the transverse crest tends to form an acute angle with the mesial protoconid ridge and the lingual cusp is placed slightly mesial or opposite to the buccal cusp (Suwa, 1990; Suwa et al., 1996; Delezene and Kimbel, 2011). Thus, the distal location of lingual cusp in some post-*habilis Homo* as well as *H. floresiensis* P_3s is a secondary acquisition of the primitive pattern that is derived compared to *H. habilis*. In support of this view, these Pleistocene *Homo* P_3s also lack other plesiomorphic features present in early Pliocene hominins such as an obliquely elongated crown shape (strong mesiobuccal protrusion of the buccal face) and sharp occlusal crests (Suwa et al., 1996; Delezene and Kimbel, 2011). Although the transverse crests of the *H. floresiensis* P_3s have lost their edges by wear, the unworn portions clearly show that these crests have thick bases.

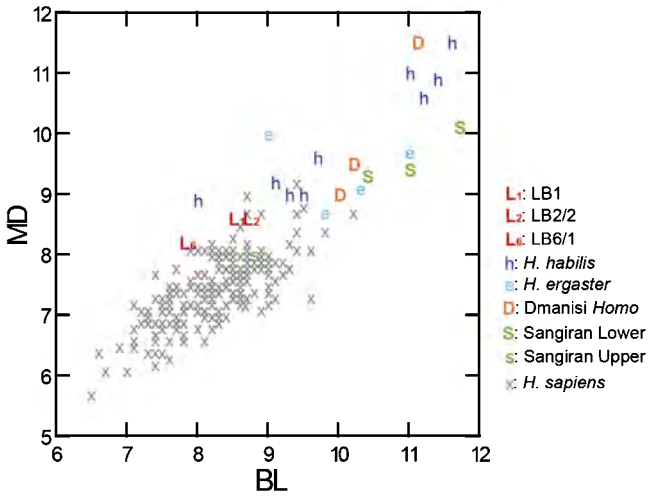

Figure 8. Scatter plot of P_3 MD and BL crown diameters (mm). The fossil comparative specimens included are as follows: *H. habilis sensu lato*: Omo 29-43, Omo 75-14, KNM-ER 1802, KNM-ER 60000 (Leakey et al., 2012); OH 6, OH 7, OH 13, OH 16, OH 68 (Clarke, 2012); *H. ergaster*: KNM-ER 992, KNM-ER 1814, KNM-ER 1808, KNM-WT 15000; Dmanisi *Homo*: D211, D2735, D2600 (Martinón-Torres et al., 2008); Sangiran Lower: S 6a, S 9, S 22; Sangiran Upper: S 7-25. Measurements for the above fossil specimens were taken by Y.K. based on high-quality plaster casts produced from the original specimens by Y.K. or Gen Suwa, or from the literature. The *H. sapiens* is a global sample from Asia, Oceania, Europe, and Africa, and is based on high-quality plaster casts prepared by Y.K (n = 208).

The *H. floresiensis* P_3s are, however, unique, showing the beveled, generally flat but wrinkled mesiolingual occlusal surface as described above. This feature is associated with a low, mesially restricted Mmr. It is different to the 'open' anterior fovea frequently seen in *Australopithecus* as well as archaic and modern *Homo* P_3s, where a distinctly elevated Mmr is deeply incised by a furrow emanating from the pit-like anterior fovea, and is not associated with fine enamel wrinkling (e.g., Johanson et al., 1982; Tobias, 1991; Grine and Franzen, 1994). In Table 2, we compare MD dimensional proportions of P_3 within the postcanine tooth row, i.e. $P_3/(P_3 - M_2)$ or $P_3/(P_3 + M_1 + M_2)$. This comparison indicates that the relative P_3 lengths tend to be smaller in *H. sapiens*, moderately large in the Early–Middle Pleistocene *Homo* particularly in post-*habilis Homo* taxa, and extremely large in *H. floresiensis*. The metric data reported by Wolpoff (1971) also show that P_3/M_1 size ratio is higher in *H. erectus* and Neanderthals than in *H. sapiens*.

To summarize, *H. floresiensis* P_3 exhibits a primitive crown shape but is derived from *H. habilis* in cuspal arrangement, and is unique in its relatively large size and the beveled and wrinkled mesiolingual crown.

Mandibular premolar root

Brown and Maeda (2009) emphasized that the bifurcated or Tomes' mandibular premolar root forms seen in *H. floresiensis* are rare in *H. sapiens* (Shields, 2005). We agree that the roots of these (and anterior) teeth of *H. floresiensis* are robust and primitive, although we found that the P_4 roots of LB1 and LB6/1 are not bifurcated but should be described as Tomes' form with a mesiobuccal cleft (see above).

Brown and Maeda (2009) suggested that such 'complex' root forms are more frequently observed in *Australopithecus* and East African early *Homo* than in Sangiran *H. erectus* (their Table 3). This is incorrect. Observed frequencies of double-rooted mandibular premolars do not significantly differ between *H. habilis* (4/13 (P_3) and 5/10 (P_4)) (Suwa, 1990; Tobias, 1991; Wood, 1991; Leakey et al., 2012) and the older Sangiran *H. erectus* (3/6 (P_3) and 4/6 (P_4)) (Kaifu et al., 2005b). Single-rooted mandibular premolars do exist in *H. habilis* (e.g. KNM-ER 1483, 1501; OH37: Wood, 1991), and non-double-rooted P_3s from Sangiran include Tomes' root form (S 6a, S 22: Weidenreich, 1945; Kaifu et al., 2005a). Thus, the available limited information about

mandibular premolar root form is not very useful to discuss the evolutionary origin of *H. floresiensis*. More detailed morphometric analyses are needed to investigate detailed evolutionary changes in root morphology of the Pleistocene *Homo* (e.g. Kupczik and Hublin, 2010; Emonet et al., 2012; Le Cabec et al., 2013).

Molar crown shape

Jacob et al. (2006) listed the following molar traits of LB1 as evidence to link this individual with a modern 'pygmy population' from Flores: (1) a tendency for the longitudinal fissure to shift away from the buccolingual axis on mandibular molars, (2) rhomboid outlines of upper molars reflecting hypocone reduction, and (3) squared lower molar outlines related to hypoconulid loss.

The meaning of the first point is not clear to us. In our observation, the longitudinal fissures of LB1 and LB6/1 are remarkable in that their distal segments are shifted extremely lingually. This trait is more frequently found in the Early Pleistocene *Homo* than in *H. sapiens*, although this observation needs to be verified metrically in future studies. We will numerically examine the second and third points elsewhere, but we here note that it is metacone, not hypocone, that shows marked reduction on the M^1 and M^2 of LB1. We confirmed that the mandibular molars of the two *H. floresiensis* individuals are four-cusped teeth with no hypoconulid. Four-cusped M_1s and M_2s have been unknown among *H. erectus* assemblages from Indonesia and China (Martinón-Torres et al., 2007). This morphology is also rare among the Middle–Late Pleistocene European archaic *Homo* (Martinón-Torres et al., 2012). However, Zanolli (2013) recently reported four four-cusped M_2s that may have been derived from the terminal Early Pleistocene Bapang (Kabuh) Formation in the Sangiran Dome, Central Java (chronology based on Hyodo et al., 2011). Four-cusped M_2s are relatively common in modern human populations (24%), but four-cusped M_1s are rare (1%) (calculated from the data based on a large global modern human sample (n = 6790–8638) in Scott and Turner, 1997: Appendix A). Therefore, the condition in *H. floresiensis* (both of the existing two individuals have four-cusped M_1 and M_2) is not a typical observation even for *H. sapiens*. In consideration of a report that the loss of hypoconulid is correlated with the reduction in mandibular molar size in *H. sapiens* (Scott and Turner, 1997), it is possible that *H. floresiensis* independently lost the hypoconulid in association with the reduction of their mandibular molars.

Molar size sequence

During the course of the *Homo* evolution, the posterior molars experienced more marked size reduction than in the first molar, resulted in alteration of the molar size sequence within a dentition, from plesiomorphic 'M1 < M2 ≥ M3' to 'M1 > M2 > M3' (Wolpoff, 1971; Bermúdez de Castro and Nicolás, 1995; Kaifu et al., 2005b; Kaifu, 2006). The maxillary and mandibular molar size in *H. floresiensis* decreases posteriorly (M1 ≥ M2 > M3). This is a derived character seen in post-*habilis* grade *Homo* (Brown et al., 2004).

Mandibular dental arcade shape

Dental arcade shape, which became wider during hominin evolution, is a useful character for taxonomic purposes (Rosas and Bermudez de Castro, 1998; Kaifu et al., 2005b; Spoor et al., 2015; Villmoare et al., 2015). Brown and Maeda (2009) suggested that the narrow dental arcades seen in the LB1 and LB6/1 mandibles are shared with pre-1.7 Ma *Homo* and *Australopithecus* but not present or very uncommon in Asian *H. erectus* or later *Homo*. This view has been disproved by a later metric reinvestigation, which showed that their arcades are actually wider than seen in *H. habilis* or Dmanisi *Homo*, and are similar to early *H. erectus* from Java (Kaifu et al., 2011).

Conclusions

In this paper, we described the dental morphology of *H. floresiensis* and corrected some previously reported information (e.g. I^2 size, I^2/C diastema, relative C_1 size, P_3 crown dimensions, and P_4 root form). The dental assemblage of Liang Bua *H. floresiensis* represents probably five (but possibly four or six) individuals. They share similar dental morphologies and represent a single population. We also investigated primitive and modern aspects of the *H. floresiensis* teeth by reassessing the previously reported such characters.

H. floresiensis is primitive compared to *H. sapiens* in having a MD elongated P_3 crown. Other possibly archaic features of *H. floresiensis* mentioned in the present paper include a prominent canine lingual median ridge, thickening of the buccal cervical enamel on C_1 and P_3, a robust anterior tooth root, a relatively complex and robust premolar root morphology, and a squarish maxillary dental arcade. *H. floresiensis* is derived relative to *H. habilis s.l.* in having a distally located P_3 lingual cusp, comparatively wider mandibular dental arcade, four-cusped mandibular molars, posteriorly decreasing molar size sequence, and a small tooth size. The previously suggested very primitive features shared with *Australopithecus afarensis*, such as a small I^2 and presence of I^2/C diastema, are actually not evident in the existing *H. floresiensis* fossil collection. On the other hand, the teeth of *H. floresiensis* are unique, showing an extremely large relative size and mesiolingually beveled and wrinkled morphology of the P_3 crown.

As in the cases of other skeletal elements (Brown et al., 2004; Morwood et al., 2005; Larson et al., 2009; Brown and Maeda, 2009; Jungers et al., 2009b; Kaifu et al., 2011), the teeth of *H. floresiensis* exhibit an impressive mosaic of primitive, derived, and unique characters. The derived characters include four-cusped mandibular molars, a trait that can be described as modern, like *H. sapiens*. The primitive features include those comparable to some of the Early Pleistocene *Homo* (P_3 crown shape, P_3 root morphology, and mandibular dental arcade). The dental morphology of *H. floresiensis* has been controversial: some researchers view that it is fully modern (Jacob et al., 2006), whereas others point out a few very primitive features that suggest an evolutionary link with *H. habilis s.l.* or *Australopithecus* (Brown et al., 2004; Brown and Maeda, 2009). Although more comprehensive comparative analyses are needed to fully illustrate the dental morphological affinities of this dwarfed hominin species, the present study found no grounds for both of these conflicting views.

Acknowledgments

We are grateful to Gen Suwa for the micro-CT scanning of LB1, and Gen Suwa, Tony Djubiantono, Ian Tattersall, Ken Mowbray, John de Vos, Philippe Mennecier, Fabrice Demeter, Nguyen Kim Thuy, and Nguyen Lan Cuong for access to the specimens in their care. Y.K. thanks the late Mike Morwood for his invitation and kind support for this project. This study was supported by grants from the Japan Society for the Promotion of Science (No. 24247044) and the National Museum of Nature and Science, Tokyo, to Y.K.

References

Aiello L.C. (2010) Five years of *Homo floresiensis*. American Journal of Physical Anthropology, 142: 167–179.

Antón S.C. (2003) Natural history of *Homo erectus*. Yearbook of Physical Anthropology, 46: 126–170.

Argue D., Donlon D., Groves C., and Wright R. (2006) *Homo floresiensis*: microcephalic, pygmoid, *Australopithecus* or *Homo*? Journal of Human Evolution, 51: 360–374.

Argue D., Morwood M., Sutikna T., Jatmiko, and Saptomo E.W. (2009) *Homo floresiensis*: a cladistic analysis. Journal of Human Evolution, 57: 623–639.

Baab K.L. and McNulty K.P. (2009) Size, shape, and asymmetry in fossil hominins: The status of the LB1 cranium based on 3D morphometric analyses. Journal of Human Evolution, 57: 608–622.

Baab K.L., McNulty K.P., and Harvati K. (2013) *Homo floresiensis* contextualized: a geometric morphometric comparative analysis of fossil and pathological human samples. PLoS ONE, 8(7): e69119. doi:10.1371/journal.pone.0069119.

Baccetti T. (1998) Tooth rotation associated with aplasia of nonadjacent teeth. The Angle Orthodontist, 68: 471–474.

Bailey S.E., Skinner M.M., and Hublin J.-J. (2011) What lies beneath? An evaluation of lower molar trigonid crest patterns based on both dentine and enamel expression. American Journal of Physical Anthropology, 145: 505–518.

Bermúdez de Castro J.M. and Nicolás M.E. 1995. Posterior dental size reduction in hominids: the Atapuerca evidence. American Journal of Physical Anthropology, 96: 335–356.

Bermúdez de Castro J.M., Rosas A., and Nicolás M.E. (1999) Dental remains from Atapuerca-TD6 (Gran Dolina site, Burgos, Spain). Journal of Human Evolution, 37: 523–566.

Bermúdez de Castro J.M., Martinón-Torres M., Gómez-Robles A., Prado L., and Sarmiento S. (2007) Comparative analysis of the Gran Dolina-TD6 (Spain) and Tighennif (Algeria) hominin mandibles. Bulletins et Mémoires de la Société d'Anthropologie de Paris, 19: 149–167.

Brown B. and Walker A. (1993) The dentition. In: Walker A. and Leakey R. (eds.), The Nariokotome *Homo erectus* Skeleton. Harvard University Press, Cambridge, MA, pp. 161–192.

Brown P. (2012) LB1 and LB6 *Homo floresiensis* are not modern human (*Homo sapiens*) cretins. Journal of Human Evolution, 62: 201–224.

Brown P. and Maeda T. (2009) Liang Bua *Homo floresiensis* mandibles and mandibular teeth: a contribution to the comparative morphology of a new hominin species. Journal of Human Evolution, 57: 571–596.

Brown P., Sutikna T., Morwood M.J., Soejono R.P., Jatmiko, Saptomo E.W., and Rokus Awe Due (2004) A new small-bodied hominin from the Late Pleistocene of Flores, Indonesia. Nature, 431: 1055–1061.

Carbonell E., Bermudez de Castro J.M., Arsuaga J.L., Allue E., Bastir M., Benito A., Caceres I., Canals T., Diez J.C., van der Made J., Mosquera M., Olle A., Perez-Gonzalez A., Rodriguez J., Rodriguez X.P., Rosas A., Rosell J., Sala R., Vallverdu J., and Verges J.M. (2005) An Early Pleistocene hominin mandible from Atapuerca-TD6, Spain. Proceedings of the National Academy of Sciences, USA, 102: 5674–5678.

Clarke R.J. (2012) A *Homo habilis* maxilla and other newly-discovered hominid fossils from Olduvai Gorge, Tanzania. Journal of Human Evolution, 63: 418–428.

Daegling D.J., Patel B.A., and Jungers W.L. (2014) Geometric properties and comparative biomechanics of *Homo floresiensis* mandibles. Journal of Human Evolution, 68: 36–46.

Delezene L.K. and Kimbel W.H. (2011) Evolution of the mandibular third premolar crown in *Australopithecus*. Journal of Human Evolution, 60: 711–730.

Emonet E.-G., Tafforeau P., Chaimanee Y., Guy F., de Bonis L., Koufos G., and Jaeger J.-J. (2012) Three-dimensional analysis of mandibular dental root morphology in hominoids. Journal of Human Evolution, 62: 146–154.

Falk D., Hildebolt C., Smith K., Morwood M.J., Sutikna T., Brown P., Jatmiko, Saptomo E.W., Brunsden B., and Prior F. (2005) The brain of LB1, *Homo floresiensis*. Science, 308: 242–245.

Falk D., Hildebolt C., Smith K., Morwood M.J., Sutikna T., Jatmiko, Saptomo E.W., and Prior F. (2009) LB1's virtual endocast, microcephaly, and hominin brain evolution. Journal of Human Evolution, 57: 597–607.

Gordon A.D., Nevell L., and Wood B. (2008) The *Homo floresiensis* cranium (LB1): Size, scaling and early *Homo* affinities. Proceedings of the National Academy of Sciences, USA, 105: 4650–4655.

Grine F.E. and Franzen J.L. (1994) Fossil hominid teeth from the Sangiran Dome (Java, Indonesia). Courier Forsch Senckenberg, 171: 75–103.

Henneberg M. and Schofield J. (2008) The Hobbit Trap. Wakefield, Kent Town, South Australia.

Hershkovitz I., Kornreich L., and Laron Z. (2007) Comparative skeletal features between *Homo floresiensis* and patients with primary growth hormone insensitivity (Laron Syndrome). American Journal of Physical Anthropology, 134: 198–208.

Hillson S., FitzGerald C., and Flinn H. (2005) Alternative dental measurements: proposals and relationships with other measurements. American Journal of Physical Anthropology, 126: 413–426.

Holliday T.W. and Franciscus R.G. (2009) Body size and its consequences: allometry and the lower limb length of Liang Bua 1 (*Homo floresiensis*). Journal of Human Evolution, 57: 223–228.

Holliday T.W. and Franciscus R.G. (2012) Humeral length allometry in African hominids (sensu lato) with special reference to A.L. 288-1 and Liang Bua 1. PaleoAnthropology, 2012: 1–12.

Hyodo M., Matsu'ura S., Kamishima Y., Kondo M., Takeshita Y., Kitaba I., Danhara T., Aziz F., Kurniawan I., and Kumai H. (2011) High-resolution record of the Matuyama–Brunhes transition constrains the age of Javanese *Homo erectus* in the Sangiran dome, Indonesia. Proceedings of the National Academy of Sciences, USA, 108: 19563–19568.

Jacob T., Indriati E., Soejono R.P., Hsü K., Frayer D.W., Eckhardt R.B., Kuperavage A.J., Thorne A., and Henneberg M. (2006) Pygmoid Australomelanesian *Homo sapiens* skeletal remains from Liang Bua, Flores: population affinities and pathological abnormalities. Proceedings of the National Academy of Sciences, USA, 103: 13421–13426.

Johanson D.C., White T.D., and Coppens Y. (1982) Dental remains from the Hadar Formation, Ethiopia: 1974–1977 collection. American Journal of Physical Anthropology, 57: 545–603.

Jungers W.L. (2013) *Homo floresiensis*. In: Begun D.R. (ed.), A Companion to Paleoanthropology. Blackwell, Oxford, pp. 584–600.

Jungers W.L. and Kaifu Y. (2011) On dental wear, dental work, and oral health in the type specimen (LB1) of *Homo floresiensis*. American Journal of Physical Anthropology, 145: 282–289.

Jungers W.L., Harcourt-Smith W.E.H., Wunderlich R.E., Tocheri M.W., Larson S.G., Sutikna T., Rokhus Due Awe, and Morwood, M.J. (2009a) The foot of *Homo floresiensis*.

Nature, 495: 81–84.
Jungers W.L., Larson S.G., Harcourt-Smith W., Morwood M.J., Sutikna T., Rokhus Due Awe, and Djubiantono T. (2009b) Descriptions of the lower limb skeleton of *Homo floresiensis*. Journal of Human Evolution, 57: 538–554.
Kaifu Y. (2006) Advanced dental reduction in Javanese *Homo erectus*. Anthropological Science, 114: 35–43.
Kaifu Y., Aziz F., and Baba H. (2005a) Hominid mandibular remains from Sangiran: 1952–1986 collection. American Journal of Physical Anthropology, 128: 497–519.
Kaifu Y., Baba H., Aziz F., Indriati E., Schrenk F., and Jacob T. (2005b) Taxonomic affinities and evolutionary history of the Early Pleistocene hominids of Java: dentognathic evidence. American Journal of Physical Anthropology, 128: 709–726.
Kaifu Y., Baba H., Kurniawan I., Sutikna T., Saptomo E.W., Jatmiko, Rokhus Due Awe, Kaneko T., Aziz F., and Djubiantono T. (2009) Brief communication: "Pathological" deformation in the skull of LB1, the type specimen of *Homo floresiensis*. American Journal of Physical Anthropology, 140: 177–185.
Kaifu Y., Kaneko T., Kurniawan I., Sutikna T., Saptomo E.W., Jatmiko, Rokhus Due Awe, Aziz F., Baba H., and Djubiantono T. (2010) Posterior deformational plagiocephaly properly explains the cranial asymmetries in LB1: a reply to Eckhardt and Henneberg. American Journal of Physical Anthropology, 143: 335–336.
Kaifu Y., Baba H., Sutikna T., Morwood M., Kubo D., Saptomo E.W., Jatmiko, Due Awe R., and Djubiantono T. (2011) Craniofacial morphology of *Homo floresiensis*: description, taxonomic affinities, and evolutionary implication. Journal of Human Evolution, 61: 644–682.
Kimbel W.H. and Delezene L.K. (2009) Lucy's 'Redux': a review of research on Australopithecus afarensis. Yearbook of Physical Anthropology, 52: 2–48.
Kubo D., Kono R.T., Saso A., Mizushima S., and Suwa G. (2008) Accuracy and precision of CT-based endocranial capacity estimations: a comparison with the conventional millet seed method and application to the Minatogawa 1 skull. Anthropological Science, 116: 77–85.
Kubo D., Kono R.T., and Kaifu Y. (2013) Brain size of *Homo floresiensis* and its evolutionary implications. Proceedings of the Royal Society B, 280: 20130338.
Kupczik K. and Hublin J.-J. (2010) Mandibular molar root morphology in Neanderthals and Late Pleistocene and recent *Homo sapiens*. Journal of Human Evolution, 59: 525–541.
Larson S.G., Jungers W., Morwood M.J., Sutikna T., Jatmiko, Wahyu Saptomo E., Rokhus Due Awe, and Djubiantono T. (2007) *Homo floresiensis* and the evolution of hominin shoulder. Journal of Human Evolution, 53: 718–731.
Larson S.G., Jungers W., Tocheri M.W., Orr C.M., Morwood M.J., Sutikna T., Rokhus Due Awe, and Djubiantono T. (2009) Descriptions of the upper limb skeleton of *Homo floresiensis*. Journal of Human Evolution, 57: 555–570.
Leakey M.G., Spoor F., Dean M.C., Feibel C.S., Antón S., Kiarie C., and Leakey, L.N. (2012) New fossils from Koobi Fora in northern Kenya confirm taxonomic diversity in early *Homo*. Nature, 488: 201–204.
Le Cabec A., Gunz P., Kupczik K., Braga J., and Hublin, J.-J. (2013) Anterior tooth root morphology and size in Neanderthals: taxonomic and functional implications. Journal of Human Evolution, 64: 169–193.
Lukacs J.R., Nelson G.C., and Walker C. (2006) Anomalies of dental development in modern humans and *Homo floresiensis*. American Journal of Physical Anthropology, Supple. 42: 122–123.
Lyras G.A., Dermitzakis M.D., van der Geer A.A.E., and de Vos J. (2009) The origin of *Homo floresiensis* and its relation to evolutionary processes under isolation. Anthropological Science, 117: 33–43.
Martínez de Pinillos M., Martinón-Torres M., Skinner M.M., Arsuaga J.L., Gracia-Téllez A., Martínez I., Martín-Francés L., and Bermúdez de Castro J.M. (2014) Trigonid crests expression in Atapuerca-Sima de los Huesos lower molars: Internal and external morphological expression and evolutionary inferences. Comptes Rendus Palevol, 13: 205–221.
Martinón-Torres M., Bermúdez de Castro J.M., Gómez-Robles A., Arsuaga J.L., Carbonell E., Lordkipanidze D., Manzi G., and Margvelashvili A. (2007) Dental evidence on the hominin dispersals during the Pleistocene. Proceedings of the National Academy of Sciences, USA, 104: 13279–13282.
Martinón-Torres M., Bermúdez de Castro J.M., Gómez-Robles A., Margvelashvili A., Prado L., Lordkipanidze D., and Vekua A. (2008) Dental remains from Dmanisi (Republic of Georgia): morphological analysis and comparative study. Journal of Human Evolution, 55: 249–273.
Martinón-Torres M., Bermúdez de Castro J.M., Gómez-Robles A., Prado-Simón L., and Arsuaga J.A. (2012) Morphological description and comparison of the dental remains from Atapuerca-Sima de los Huesos site (Spain). Journal of Human Evolution, 62: 7–58.
Morwood M.J. and Jungers W.L. (2009) Conclusions: implications of the Liang Bua excavations for hominin evolution and biogeography. Journal of Human Evolution, 57: 640–648.
Morwood M.J., Soejono R.P., Roberts R.G., Sutikna T., Turney C.S.M., Westaway K.E., Rink W.J., Zhao J.-x., van den Bergh G.D., Rokus Awe Due, Hobbs D.R., Moore M.W., Bird M.I., and Fifield L.K. (2004) Archaeology and age of *Homo floresiensis*, a new hominin from Flores in eastern Indonesia. Nature, 431: 1087–1091.
Morwood M.J., Brown P., Jatmiko, Sutikna T., Saptomo E.W., Westaway K.E., Rokus Awe Due, Roberts R.G., Maeda T., Wasisto S., and Djubiantono T. (2005) Further evidence for small-bodied hominins from the late pleistocene of Flores, Indonesia. Nature, 437: 1012–1017.
Morwood M.J., Sutikna T., Saptomo E.W., Jatmiko, Hobbs D.R., and Westaway K.E. (2009) Preface: research at Liang Bua, Flores, Indonesia. Journal of Human Evolution, 57: 437–449.
Natsume A., Koyasu K., Oda S., Nakagaki H., and Hanamura H. (2006) Premolar and molar rotation in wild Japanese serow populations on Honshu Island, Japan. Archives of Oral Biology, 51: 1040–1047.
Obendorf P.J., Oxnard C.E., and Kefford B.J. (2008) Are the small human-like fossils found on Flores human endemic cretins? Proceedings of the Royal Society B, 275, 1287–1296.
Orr C.M., Tocheri M.W., Burnett S.E., Awe R.D., Saptomo E.W., Sutikna T., Jatmiko, Wasisto S., Morwood M.J., and Jungers W.L. (2013) New wrist bones of *Homo floresiensis* from Liang Bua (Flores, Indonesia). Journal of Human Evolution, 64: 109–129.
Rightmire G.P. (1980) Middle Pleistocene hominids from Olduvai Gorge, northern Tanzania. American Journal of Physical Anthropology, 53: 225–241.
Rightmire G.P., Lordkipanidze D., and Vekua A. (2006) Anatomical descriptions, comparative studies and evolutionary significance of the hominin skulls from Dmanisi, Republic of Georgia. Journal of Human Evolution, 50: 115–141.
Rosas A. and Bermudez de Castro J.M. (1998) On the taxonomic affinities of the Dmanisi mandible (Georgia). American Journal of Physical Anthropology, 107: 145–162.
Scott G.R. and Turner C.G., II (1997) Anthropology of Modern Human Teeth. Cambridge University Press, Cambridge.
Shields E.D. (2005) Mandibular premolar and second molar root morphological variation in modern humans: what root number can tell us about tooth morphogenesis. American Journal of Physical Anthropology, 128: 299–311.
Smith B.H. (1984) Patterns of molar wear in hunter-gatherers and agriculturists. American Journal of Physical Anthropology, 63: 39–56.
Spoor F., Gunz P., Neubauer S., Stelzer S., Scott N., Kwekason A., and Dean C.M. (2015) Reconstructed *Homo habilis* type OH

7 suggests deep-rooted species diversity in early *Homo*. Nature, 519: 83–86.
Suwa G. (1990) A comparative analysis of hominid dental remains from the Shungra and Usno Formations, Omo Valley, Ethiopia. PhD dissertation. University of California, Berkeley.
Suwa G., White T., and Howell F.C. (1996) Mandibular postcanine dentition from the Shungra Formation, Ethiopia: crown morphology, taxonomic allocations, and Plio-Pleistocene hominid evolution. American Journal of Physical Anthropology, 101: 247–282.
Suwa G., Asfaw B., Haile-Selassie Y., White T., Katoh S., WoldeGabriel G., Hart W.K., Nakaya H., and Beyene Y. (2007) Early Pleistocene *Homo erectus* fossils from Konso, southern Ethiopia. Anthropological Science, 115: 133–151.
Suwa G., Kono R.T., Simpson S.W., Asfaw B., Lovejoy C.O., and White T. (2009) Paleobiolofical implications of the *Ardipithecus ramidus* dentition. Science, 326: 94–99.
Suwa G., Fukase H., Kono R.T., Kubo D., and Fujita M. (2011) Mandibular tooth root size in modern Japanese, prehistoric Jomon, and Late Pleistocene Minatogawa human fossils. Anthropological Science, 119: 159–171.
Tobias P.V. (1991) Olduvai Gorge, 4: The Skulls, Endocasts and Teeth of *Homo habilis*. Cambridge University Press, Cambridge.
Tocheri M.W., Orr C.M., Larson S.G., Sutikna T., Jatmiko, Saptomo E.W., Rokus Awe Due, Djubiantono T., Morwood M.J., and Jungers W.L. (2007) The primitive wrist of *Homo floresiensis* and its implications for hominin evolution. Science, 317: 1743–1745.
Turner C.G., II, Nichol C.R., and Scott G.R. (1991) Scoring procedures for key morphological traits of the permanent dentition: the Arizona State University dental anthropology system. In: Kelley M. and Larsen C. (eds.), Advances in Dental Anthropology. Wiley-Liss, New York, pp. 13–31.
van Heteren A.H. (2012) The hominins of Flores: insular adaptation of the lower body. Comptes Rendu Palevol, 11: 169–179.
Villmoare B., Kimbel W.H., Seyoum C., Campisano C.J., DiMaggio E., Rowan J., Braun D.R., Arrowsmith J.R., and Reed K.E. (2015) Early *Homo* at 2.8 Ma from Ledi-Geraru, Afar, Ethiopia. Science, 347: 1352–1355.
Ward C.V., Leakey M.G., and Walker A. (2001) Morphology of *Australopithecus anamensis* from Kanapoi and Allia Bay, Kenya. Journal of Human Evolution, 41: 255–368.
Ward C.V., Manthi F.K., and Plavcan J.M. (2013) New fossils of *Australopithecus anamensis* from Kanapoi, West Turkana, Kenya (2003–2008). Journal of Human Evolution, 65: 501–524.
Weidenreich F. (1937) The dentition of *Sinanthropus pekinensis*: a comparative odontography of the hominids. Paleontologica Sinica, New Series D, 1: 1–180.
Weidenreich F. (1945) Giant early man from Java and South China. Anthropological Papers of the American Museum of Natural History, 40: 1–134.
White T.D., Johandon D.C., and Kimbel W.H. (1981) *Australopithecus africanus*: its phyletic position reconsidered. South African Journal of Science, 77: 445–470.
Wolpoff M.H. (1971) Metric Trends in Hominid Dental Evolution. Case Western Reserve University Studies in Anthropology, 2.
Wood B.A. (1991) Koobi Fora Research Project, 4: Hominin Cranial Remains from Koobi Fora. Clarendon Press, Oxford.
Wood B.A. and Uytterschaut H. (1988) Analysis of the dental morphology of Plio-Pleistocene hominids. III. Mandibular premolar crowns. Journal of Anatomy, 154: 121–156.
Wood B.A., Abbott S.A., and Uyttershaut H. (1988) Analysis of the dental morphology of Plio-Pleistocene hominids. IV. Mandibular postcanine root morphology. Journal of Anatomy, 156: 107–139.
Zanolli C. (2013) Additional evidence for morpho-dimensional tooth crown variation in a new Indonesian *H. erectus* sample from the Sangiran Dome (Central Java). PLoS One, 8(7): e67233, doi:10.1371/journal.pone.0067233.